journal of the mechanical behavior of biomedical materials 104 (2020) 103659

Contents lists available at ScienceDirect

Journal of the Mechanical Behavior of Biomedical Materials

journal homepage: http://www.elsevier.com/locate/jmbbm

Aging resistance of an experimental zirconia-toughened alumina composite for large span dental prostheses: Optical and mechanical characterization

E.B. Benalcázar Jalkh [a,e,*], E.T.P. Bergamo [a], K.N. Monteiro [b], P.F. Cesar [b], L.A. Genova [c], A.C. O. Lopes [a], P.N. Lisboa Filho [d], P.G. Coelho [e,f,g], C.F. Santos [h], F. Bortolin [a], M.M.T. Piza [a], E. A. Bonfante [a]

[a] Department of Prosthodontics and Periodontology, University of São Paulo - Bauru School of Dentistry, Bauru, SP, Brazil
[b] Department of Biomaterials and Oral Biology, University of São Paulo, School of Dentistry, SP, Brazil
[c] Nuclear and Energy Research Institute, SP, Brazil
[d] Department of Physics, São Paulo State University, Bauru, SP, Brazil
[e] Department of Biomaterials and Biomimetics, New York University College of Dentistry, New York, NY, USA
[f] Hansjörg Wyss Department of Plastic Surgery, NYU Langone Medical Center, New York, NY, USA
[g] Mechanical and Aerospace Engineering, NYU Tandon School of Engineering, New York, NY, USA
[h] Department of Biological Sciences, Discipline of Pharmacology, University of São Paulo, Bauru School of Dentistry, SP, Brazil

ARTICLE INFO

Keywords:
Ceramics
Alumina
Zirconia
Microstructure
Mechanical properties
Optical properties

ABSTRACT

Purpose: To synthesize a zirconia-toughened alumina (ZTA) composite with 85% alumina matrix reinforced by 15% zirconia and to characterize its optical and mechanical properties before and after artificial aging, to be compared with a conventional dental zirconia (3Y-TZP).

Material and methods: After syntheses, ZTA and 3Y-TZP powders were uniaxially and isostatically pressed. Green-body samples were sintered and polished to obtain 80 disc-shaped specimens per group (12 × 1 mm, ISO 6872:2015). The crystalline content and microstructure were characterized by X-ray diffraction (XRD) and scanning electron microscope (SEM). Optical properties were determined by the calculation of contrast ratio (CR) and translucency parameter (TP) using reflectance data. Mechanical properties were assessed by Vickers hardness, fracture toughness and biaxial flexural strength test (BFS). All analyses were conducted before and after artificial aging (20h, 134 °C, 0.22 MPa). Optical parameters and microhardness differences were evaluated through repeated-measures analysis of variance ($p < 0.05$). BFS data were analyzed using Weibull statistics (95% CI).

Results: The synthesis of the experimental ZTA composite was successful, with 98% of theoretical density, as shown in the SEM images. XRD patterns revealed typical zirconia and alumina crystalline phases. ZTA optical properties parameters showed no effect of aging, with a high CR and low TP values denoting a high masking-ability. 3Y-TZP presented lower masking-ability and aging significantly affected its optical properties. ZTA Vickers hardness, fracture toughness and Weibull parameters, including characteristic stress and Weibull modulus were not influenced by aging, while 3Y-TZP presented a significant decrease in characteristic stress and increase in fracture toughness after aging. The ZTA probability of survival for missions of 300 and 500 MPa was estimated at ~99% validating its use for 3-unit posterior fixed dental prostheses (FDP), and no different from conventional 3Y-TZP. At high-stress mission (800 MPa) a significant decrease in probability of survival was observed for aged 3Y-TZP (84%) and for immediate and aged ZTA (73 and 82% respectively).

Conclusion: The ZTA composite presented a dense microstructure, with preservation of the crystalline content, optical and mechanical properties after artificial aging, which encourages future research to validate its potential use for large span FDP.

* Corresponding author. Department of Prosthodontics and Periodontology, University of Sao Paulo – Bauru School of Dentistry, Al. Otávio Pinheiro Brisola 9-75, Bauru, SP, 17.012-901, Brazil.
E-mail address: ernestobenalcazarj@gmail.com (E.B. Benalcázar Jalkh).

https://doi.org/10.1016/j.jmbbm.2020.103659
Received 24 October 2019; Received in revised form 21 January 2020; Accepted 27 January 2020
Available online 28 January 2020

1. Introduction

The outstanding mechanical properties of yttria-stabilized tetragonal zirconia polycrystals (Y-TZP) rely on the transformation toughening mechanism, which is determined by the capability of tetragonal zirconia grains to undergo a stress-mediated phase transformation to monoclinic phase. This phenomenon, known as R-curve behavior yields Y-TZP the highest fracture toughness among the all-ceramic systems currently used in dentistry (Denry and Kelly, 2008). Nevertheless, Y-TZP metastability makes it susceptible to low temperature degradation (LTD), a steady and continued tetragonal to monoclinic (t-m) phase transformation due to stress and moist environment exposition (Chevalier et al., 1999). LTD may be accompanied by the appearance of micro cracks resulting from stress accumulation within the material eventually leading to loss of mechanical properties (Chevalier et al., 2009a). Critical events in the beginning of the 21st century, where hundreds of femoral head Y-TZP prostheses fractured due to LTD process, raised concerns about the long-term hydrothermal stability of zirconia as a biomedical material (Chevalier et al., 2009b).

For dental applications, Y-TZP remains in direct contact with body fluids, making it susceptible to tetragonal to monoclinic phase transformation not only due to mechanical stress, but also water presence and LTD. *In vitro* researches have reported a wide variation in phase transformation among zirconia stabilized dental materials, from 2.13% to 81.4% (Pereira et al., 2015, 2016). Such variability is dependent on several parameters including Y-TZP microstructure, grain size, manufacturing and processing methods, along with laboratory aging protocol (Pereira et al., 2015). Even when Y-TZP is used as an infrastructure material and veneered with porcelains, the moisture of the porcelain suspension and its subsequent heating during the sintering process has shown to trigger phase transformation at the porcelain/Y-TZP interface (Tholey et al., 2010). This interfacial tetragonal-to-monoclinic transformation has been suggested to compromise the strength of the prostheses due to increased residual stress within the porcelain veneer (Fukushima et al., 2014). Previous systematic reviews have reported significantly higher rates of technical complications, mainly veneering ceramic chipping, for porcelain fused to zirconia (PFZ) restorations relative to porcelain fused to metal (PFM) restorations (Pieralli et al., 2018; Sailer et al., 2016, 2018a). Moreover, the longest randomized clinical trial (10 years follow-up) has also reported higher technical complication rates for PFZ, including framework fractures, when compared with PFM fixed dental prostheses (FDP). The long term outcomes of long span zirconia still warrant more investigation (Sailer et al., 2018b).

To overcome the hydrothermal instability issues of Y-TZP at room temperature, the biomedical field has proposed the combination of zirconia and alumina particles (Chevalier, 2006; Fabbri et al., 2014). Zirconia-toughened alumina (ZTA) are polycrystalline ceramic composites commonly created by the addition of a disperse phase of Y-TZP in an alumina matrix (Gracis et al., 2015). Such combination has revealed an increase in fracture toughness through different mechanisms, including stress-induced phase transformation and compressive stress resulting from the thermal expansion mismatch of the two crystalline phases (Wang and Stevens, 1989; Sequeira et al., 2017), as well as, favorable tribochemical properties when compared to monolithic alumina. In addition, the alumina matrix contributes to the hydrothermal stability of zirconia by decreasing the LTD phenomena (Chevalier and Gremillard, 2009; Jiang et al., 2013). In fact, LTD progression is dictated by a nucleation and growth process, which can be controlled in ZTA composites through zirconia grains interconnectivity within the alumina matrix, known as percolation threshold (Pecharroman et al., 2003). Although some studies in orthopedics have shown interesting mechanical results with a weight ratio of zirconia and alumina up to 30 and 70%, respectively, they also suggested that increasing Y-TZP concentrations may favor zirconia grains interconnectivity and LTD. (Casellas et al., 1999; Karihaloo, 1991; Lange, 1982) Thus, the fraction that provided a better balance between mechanical properties and LTD control, has shown to be approximately 16% zirconia in 84% alumina matrix (Pecharromán et al., 2003).

Furthermore, polycrystalline ceramic systems usually exhibit high opacity due to the inherent birefringence associated with the prevalence of noncubic phases and light scattering from grain boundaries, pores and secondary crystal content (Krell and Klimke, 2007; Zhang and Lawn, 2017). Hence, their clinical applicability chiefly comprises infrastructure systems for porcelain-veneered prostheses (Daou, 2014). Besides the previously discussed effect of LTD on increasing residual stress at porcelain/Y-TZP interface, progressive tetragonal-to-monoclinic phase transformation has been associated with an increase in the material translucency, which may alter long-term esthetic results of zirconia-based restorations (Kim and Kim, 2018). ZTA composite hydrothermal stability may also be a very attractive alternative in such clinical scenarios.

Given the metastability of Y-TZP and potential risk for long-term complications, the present study sought to develop a synthesis method for the production of 85% alumina and| 15% zirconia ZTA composite, to perform microstructural, optical and mechanical characterization before and after artificial aging, and to compare it with a conventional Y-TZP. The postulated null hypothesis was that aging protocol would not affect the microstructure, optical and mechanical properties of the ZTA composite.

2. Material and Methods

2.1. ZTA composite syntheses and specimens preparation

The experimental zirconia-toughened alumina (ZTA) composite was synthesized through the mixture of a high-purity alumina powder (CT3000 SDP, Almatis, Frankfurt, Germany) and an yttria-stabilized tetragonal zirconia polycrystals powder (3YSB-E, Tosoh Corporation, Tokyo, Japan) in a weight ratio of 85% and 15%, respectively. The individual composition and particle size of the powders are described in Table 1.

Alumina and zirconia powders were blended in ethanol suspensions, then mixed and homogenized in a friction mill for 4 h with high-purity alumina spheres. The slurry was dried in rotary evaporator (801, Fisaton, São Paulo, Brazil) and the obtained powder was manually granulated and sieved.

Once synthesized, ZTA and 3Y-TZP powders were uniaxially pressed at 11,258 N for 30 s in a tungsten carbide matrix with 15 mm of diameter to obtain disc-shaped samples with 1.8 mm thickness. Green body discs were double wrapped and sealed in vacuum sealer (Jumbo Plus, Globavac, Itajai, SC, Brazil) and subjected to isostatic pressing (National Forge, Irvine, PA, USA) at room temperature for 30 s at 206.84 MPa.

ZTA and 3Y-TZP green body samples were then sintered at 1,600 °C and 1,500 °C respectively, for 1 h in a Zyrcomat (Vita Zahnfabrink, Bad Säckingen, Germany) furnace with heating and cooling rate of 4 °C per minute. Polishing of the two flat surfaces was performed in a semi-automatic polishing machine (Automet, 2000; Buehler, Lake Buff, IL, USA) with 220, 120, 90, 40, 25, 9, 6 and 1 μm granulated diamond disks (ALLIED High Tech Products, Rancho Dominguez, CA, USA) with diamond suspensions.

A total of eighty specimens per group with final dimensions of 12 mm of diameter and 1 mm thickness were prepared according to ISO 6872:2015 (International-Standard-Organization, 2015), and the following characterization tests were performed before and after accelerated artificial aging (20 h, 134 °C, 0.22 MPa) (Pereira et al., 2015).

2.2. Density

The theoretical density after sintering was determined based on the Archimedes' principle. The density of the specimens was measured

using an analytical balance (Adventurer Analytical balance, Ohaus, Parsippany, NJ, USA) and theoretical density kit accessory.

2.3. Scanning electron microscopy (SEM)

The microstructure of the experimental material was analyzed by scanning electron microscope (SEM, LS15 microscope, Carl Zeiss, Oberkochen, Germany). Samples were evaluated after thermal treatment at 1,500 °C during 1 h with heating and cooling rate of 4 °C per minute (Zyrcomat Furnace, Vita Zahnfabrink, Bad Säckingen, Germany). SEM images were obtained with magnifications of 5,000 to 30,000 × with a SE detector at high vacuum. An NSD-BS detector was used to assess the distribution of alumina and zirconia grains in the ZTA composite. Backscattered images were obtained in low magnification (500 and 5,000 ×).

2.4. X-ray diffraction (XRD)

Crystalline spectra were obtained by X-ray diffraction (XRD, Miniflex, Rigaku, Tokyo, Japan). The scanning was performed on the Bragg θ-2θ geometry, equipped with a graphite monochromator and Cu Kα radiation (λ = 1.5406 Å), operating at a voltage of 40 kV and a current emission of 40 mA. The data were obtained over 2θ range of 20°–70° at a scan rate of 0.2°/min and a step size of 0.020°. Characteristic zirconia and alumina peaks were identified using JCPDS-ICDD (files no. 80–789 and 81–1545). Quantitative phase analysis was carried out using the Rietveld refinement method in X'Pert HighScore software (Malvern PANalytical Ltd, Westborough, MA, USA), which estimates the weight fraction (%) of each phase based on relative peak intensity.

2.5. Optical properties

Ten specimens of ZTA were analyzed in spectrophotometer CM 3700d (Konica Minolta) that operates in the wavelengths range of visible light (400–700 nm). Contrast ratio (CR), and translucency parameter (TP) were calculated by reflectance values obtained over white (Yw) and black (Yb) background.

CR is the property that measures the transparency or opacity of the material and is measured by the reflectance ratio of the specimen on the black background (Yb) divided by the reflectance of the same specimen on a white background (Yw), which is given by Equation (1):

$$CR = Y_b / Y_w \quad (1)$$

TP, which defines the masking ability of the material, was obtained by calculating the color difference (ΔE) of the specimens on black and white backgrounds, according to equation (2):

$$\Delta E = \left[\left(L_b^* - L_w^*\right)^2 + \left(a_b^* - a_w^*\right)^2 + \left(b_b^* - b_w^*\right)^2 \right]^{1/2} \quad (2)$$

where the subscripts b* (black) and w* (white) indicate the background color, and the coordinates L*, a*, and b* correspond to the lightness, chromaticity on the red/green axis, and chromaticity on the yellow/blue axis, respectively.

2.6. Vickers hardness and fracture toughness

The surface hardness was measured based on the mean value of three Vickers impressions performed on the central surface of 10 different polished samples, with a load of 98 N and dwell time of 15 s (Reicherter Hardness tester, Buheler, Lake Bluff, IL, USA). After measuring the impressed diagonals, the Vickers hardness values were calculated by: $HV = 0.1891\ L/d^2$, where L is the load (N) and d is the arithmetic mean of the length of the two diagonals (mm). The indentation-fracture (IF) method was used to estimate the fracture toughness (K_{IC}) according to the following equation: $K_{IC} = 0.016\left(\frac{E}{HV}^{0.5}\right)\left(\frac{L}{C^{1.5}}\right)$, where L is the load (N), c is half of the median cracks, E is the elastic modulus (GPa), and HV is the hardness (Anstis et al., 1981).

2.7. Biaxial flexural strength and survival

Thirty specimens for each condition (immediate and aged) were subjected to biaxial flexural strength test (BFST) using a piston-on-three balls device, according to ISO 6872:2015. BFST was carried out in ElectroPulsTM E3000 Linear-Torsion (Instron, Norwood, MA, EUA) equipment at a crosshead speed of 0.5 mm/min until failure. The maximum load was recorded for each specimen (N), and the following equations , were used to calculate biaxial flexural strength (MPa):

$$\sigma = -0.2387\ P\ (X–Y)\ /\ b^2 \quad (3)$$

$$X = (1 + v)\ Ln\ (r_2 / r_3)^2 + ([1 - v] / 2)\ (r_2 / r_3)^2 \quad (4)$$

$$Y = (1 + v)\ (1 + Ln\ [r_1 / r_3]^2) + (1 - v)\ (r_1 / r_3)^2 \quad (5)$$

where, σ = biaxial flexural strength (MPa), P = fractured load (N), b = disk specimen thickness at fracture site (1.2 ± 0.2 mm), v = Poisson ratio (0.25), r_1 = radius of support circle (5.5 mm), r_2 = radius of loaded area (0.75 mm), and r_3 = radius of the specimen (6 mm).

The fractured specimens were examined in Axio Zoom V16 Stereo Zoom Microscope (Carl Zeiss, Oberkochen, Germany) to assess fractographic marks evidence of the fracture origin and direction of propagation.

2.8. Statistical analysis

Data from optical properties (CR and TP), Vickers hardness, and fracture toughness were tabulated and subjected to descriptive analysis, normality and homoscedasticity test. Repeated-measures analyses of variance was used for statistical evaluation of the parameters differences with an overall significance level of 5% using SPSS software (IBM SPSS Statistics version 23, Armonk, NY, USA). Data are presented as a function of estimated mean and 95% confidence interval.

Biaxial flexural strength stress data (MPa) were analyzed using Weibull 2-parameter analysis (Synthesis 9, Weibull ++9, Reliasoft, Tucson, AZ, USA). Characteristic stress (MPa) and Weibull modulus (*m*) were calculated, and a contour plot was graphed to determine differences between groups. In addition, the probability of survival as function of characteristic stress values were calculated to missions of 300, 500, and 800 MPa, which are the ISO 6872:2015 required stress for 3-unit anterior substructures (up to premolar, class 3 ceramics), 3-unit posterior substructures (class 4 ceramics), and 4-unit or larger span substructures for FDP, respectively.

Table 1
Composition and particle size of alumina and zirconia powders used in the ZTA blend.

Material	Particle Size (nm)	Powders Chemical Composition [wt.-%]						
		Y_2O_3	Al_2O_3	Na_2O	SiO_2	FeO_2O_3	CaO	MgO
3Y-TZP	90	5.35	≤0.1- 0.4	≤0.04	≤0.02	≤0.01	–	–
Alumina	600	–	99.7	0.08	0.02	0.02	0.03	0.1

3. Results

Both experimental materials exhibited a high density, exceeding 98% of their theoretical density based on the Archimedes principle.

Scanning electron microscopy images exhibited the microstructural characterization of both materials. A dense surface was obtained for the conventional 3Y-TZP and for the experimental ZTA. SEM images depicted the presence of dense spherical zirconia grains in both materials. Alumina demonstrated a higher grain size while zirconia grain growth was more restricted. Backscattered images evidenced a uniform distribution of zirconia grains within the alumina matrix. In addition, few pore and defects were observed along the ceramic surface, which may be associated to the materials processing (Fig. 1).

X-Ray diffraction (XRD) data was plotted and the spectra analysis allowed the identification of typical α-alumina and Y-TZP peaks (Fig. 2). Rietveld refinement depicted approximately 0.5% and 3.3% monoclinic content before and after autoclave aging, respectively, demonstrating ZTA aging resistance. In the other hand, 3Y-TZP spectra depicted a significant phase transformation when immediate (1%) and aged conditions were compared (12%).

The optical parameters values of both materials as a function of mean and confidence interval (CI) before and after aging are summarized in Table 2. Contrast ratio (CR) and translucency parameter (TP) corroborated with the maintenance of the optical parameters when ZTA immediate values [CR: 1.0 (0.98–1.02) and TP: 1.70 (1.4–2.0)] and aged [CR: 0.99 (0.98–1.0) and TP: 1.69 (1.49–1.89)] were compared ($p > 0.667$). Overall, the ZTA composite presented a high opacity and masking-ability, while 3Y-TZP exhibited a lower contrast ratio [0.87 (0.83–0.91)] and higher translucency parameter [7.15 (7.05–7.25)] than ZTA composite ($p < 0.001$), and 3Y-TZP optical properties were significantly affected by accelerated autoclave aging [CR: 0.78 (0.75–0.81) and TP: 10.42 (9.02–11.82)] ($p < 0.001$).

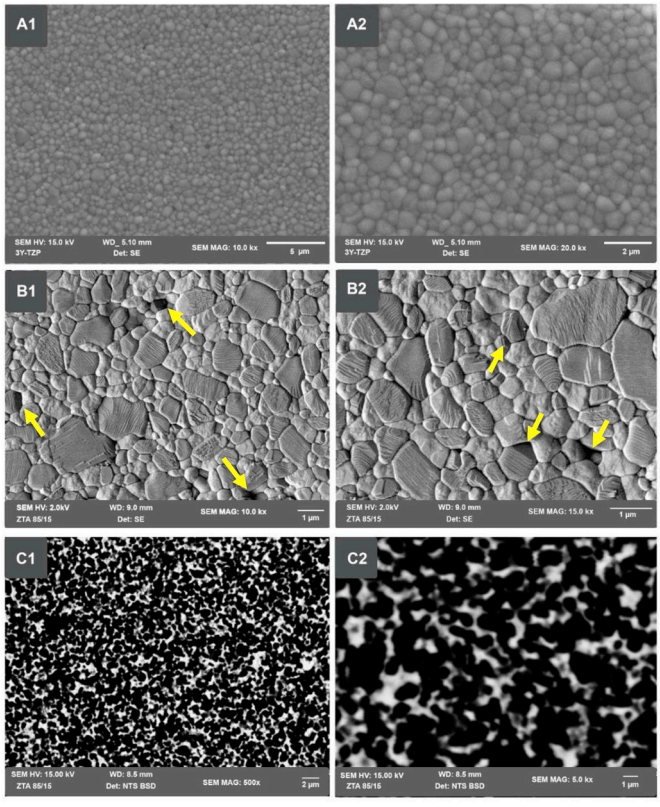

Fig. 1. (a–d). SEM images of A) 3Y-TZP at 10,000 and 20,000 × ; B) ZTA images at 10,000 and 15,000 × ; and C) Backscattered images of the ZTA composite at 500 and 5,000 × . Micrographs show the dense surface obtained for the experimental ZTA composite, with a uniform distribution of the zirconia particles within the alumina matrix. Few pores and defects can be observed (arrows).

The mechanical properties parameters of the ZTA composite and the conventional 3Y-TZP as a function of mean and 95% confidence interval before and after aging are summarized in Table 3. Higher Vickers microhardness values were found for immediate and aged ZTA when compared to the conventional Y-TZP. No statistically significant effect of aging was observed in the Vickers Hardness of both groups ($p > 0.271$). Conversely, fracture toughness of 3Y-TZP was significantly higher than ZTA composite before and after aging ($p < 0.001$), however, ZTA fracture toughness remained stable ($p = 0.082$), while fracture toughness of 3Y-TZP significantly increased after autoclave simulated LTD ($p = 0.004$).

The calculated Weibull modulus, used as a measure of the distribution of strengths that expresses the structural reliability of the material, and the characteristic stress, which represents the stress at a failure probability of approximately 63%, showed no statistical difference between immediate and aged ZTA polycrystalline composite, as demonstrated by the overlap of contours in the Contour plot (Fig. 3). Otherwise, immediate 3Y-TZP exhibited a higher characteristic stress when compared to immediate ZTA, however after aging a significant decrease was observed in 3Y-TZP's characteristic stress. The probability of survival of the experimental ZTA composite was estimated at approximately 100% for 300 and 500 MPa, however, a significant decrease up to 25% was demonstrated for immediate and aged ZTA at 800 MPa. For all estimated missions, aging did not affect the probability of survival of the ZTA composite. On the other hand, 3Y-TZP presented a probability of survival estimated at 100% for missions at 300, 500 and 800 MPa. However, aging resulted in a significant decrease, up to 20%, for missions of 800 MPa (Table 4).

Number of fractured fragments varied from two to six for both groups. Additionally, fractographic marks, including hackle lines and compression curls, were used to suggest the origin of the fracture, generally related to tensile side defects originated during the processing of the ceramic specimens, which propagated to the compression side (Fig. 4).

4. Discussion

Long-term stability of the physical-mechanical properties of biomedical materials plays a crucial role in the clinical success. For this reason, it is important not only to develop materials with high-strength but also with high degradation stability (Chevalier, 2006; Chevalier and Gremillard, 2009; Chevalier et al., 2007a). Hence, this study proposed a route for the synthesis of a zirconia-toughened alumina (ZTA) composite in a weight ratio of 85% alumina and 15% zirconia, with microstructural, optical and mechanical characterization before and after laboratory aging intended for dental applications. The synthesis of the experimental composite was successful, providing a dense microstructure and homogeneous distribution of zirconia particles within the alumina matrix. Moreover, encouraging results of optical and mechanical properties parameters, without a significant influence of artificial aging, make ZTA an attractive alternative to stabilized zirconia prostheses. Hence, the postulated null hypothesis that aging protocol would not affect the microstructure, optical and mechanical properties of the ZTA composite was accepted.

Yttria-stabilized tetragonal zirconia polycrystals (Y-TZP) systems have been extensively indicated in the clinical practice. First described by Garvie et al., in 1975, zirconia polymorphism has been studied in biomedical science because of its highlighted mechanical properties and biocompatibility (Garvie et al., 1975). Nevertheless, zirconia metastability makes it susceptible to low temperature degradation (LTD) (Chevalier, 2006; Piconi et al., 2006; Chevalier et al., 2007b). Since laboratory studies have shown large variability of monoclinic content after different aging protocols (Pereira et al., 2016), concerns have been

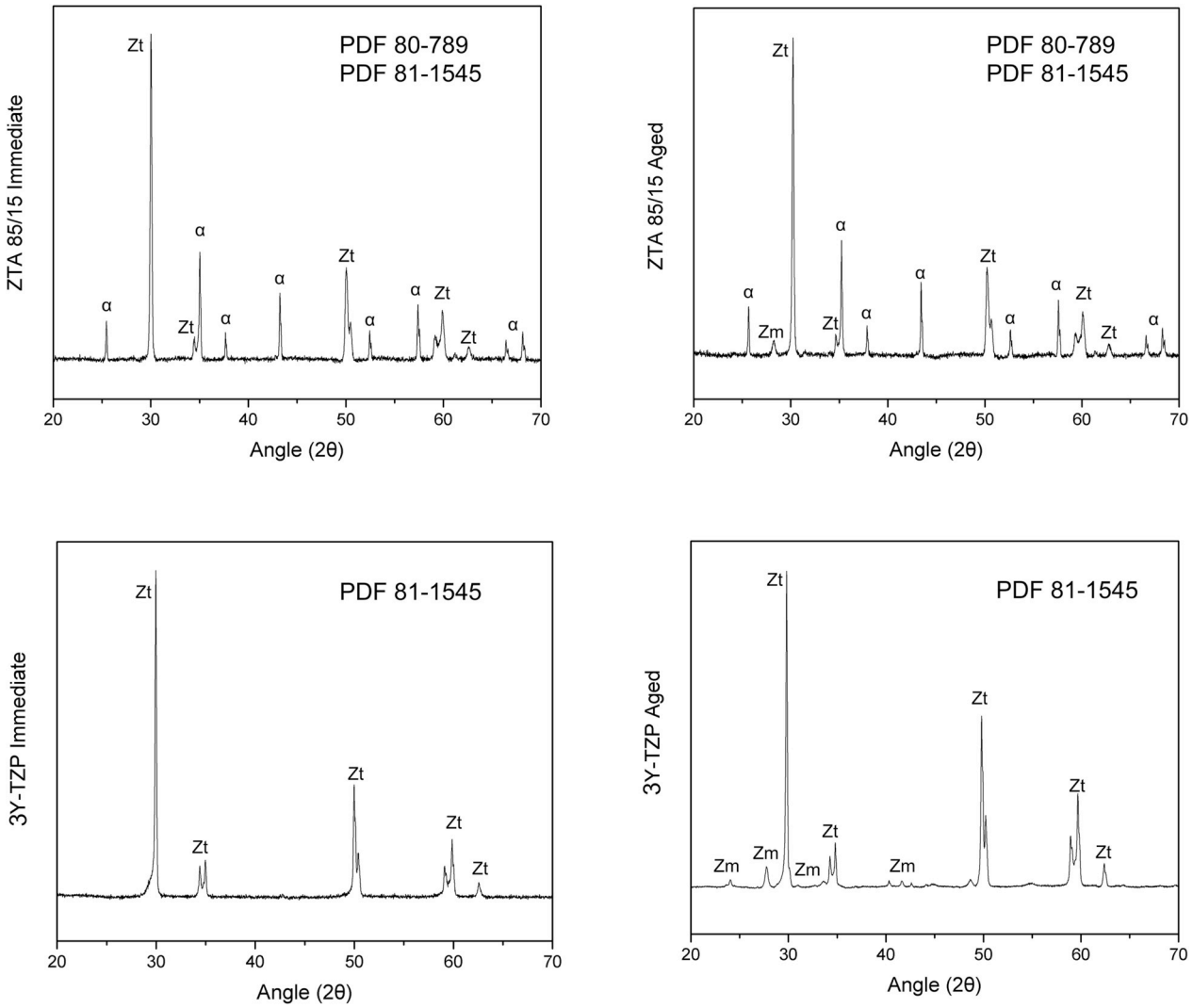

Fig. 2. XRD spectra of ZTA and 3Y-TZP composite surface before (a) and after aging (b).

Table 2
Contrast ratio (CR) and translucency parameter (TP) mean values with respective confidence intervals (CI) values.

	Contrast ratio (CR)		Translucency Parameter (TP)	
	Immediate	Aged	Immediate	Aged
ZTA	1.0 Aa (0.98–1.02)	0.99 Aa (0.98–1.0)	1.70 Aa (1.4–2.0)	1.69 Aa (1.49–1.89)
3Y-TZP	0.87 Ab (0.83–0.91)	0.78 Bb (0.75–0.81)	7.15 Ab (7.05–7.25)	10.42 Bb (9.02–11.82)

Uppercase letters denote statistically significant differences between immediate and aged groups. Lowercase letters denote significant differences between materials.

raised regarding the effects of LTD in dental prostheses. The clinical trial with longest follow-up (10 years) of porcelain fused to zirconia (PFZ) fixed dental protheses (FDP) has reported a few fractures of the zirconia framework although phase transformation quantification is yet to be confirmed (Sailer et al., 2018b). Moreover, increased residual stress has also been shown to occur due to tetragonal-to-monoclinic phase transformation at the Y-TZP/porcelain interface (Fukushima et al., 2014). The combination of the benefic properties of zirconia and alumina in a polycrystalline ceramic composite (ZTA) might provide a more hydrothermally stable and compatible alternative to Y-TZP frameworks. Hence, this study proposed a synthesis method of an experimental ZTA composite in a weight ratio of 85% alumina to 15% Y-TZP as an alternative to zirconia frameworks in all ceramic prostheses.

Microstructural analysis of the experimental ZTA composite performed by scanning electron microscope (SEM) has shown a dense surface with a uniform distribution of zirconia and alumina grains and few porosities. As alumina is the predominant phase in ZTA, the grain growth occurred more freely, while zirconia grain growth was constrained. Thereafter, it can be assumed that the mixture milling, drying, pressing, and sintering protocol have led to the achievement of a composite with a fine and homogeneous microstructure. Typical crystalline structures of zirconia, chiefly tetragonal phase, and alfa alumina were observed in the XRD spectra, as well as, an aging-resistant behavior through the preservation of the crystalline structure and a slight increase in the amount of monoclinic zirconia after aging (2.8%). A previous study of the current group has evaluated a different concentration of a ZTA composite (80% alumina and 20% zirconia), and the monoclinic content was also maintained after artificial aging (~4% increase) (Lopes et al., 2019). This behavior may lie on the limited interconnectivity of zirconia grains and higher hardness of the alumina, which restrict the

Table 3
Mean Vickers hardness, Weibull modulus and Characteristic Stress (MPa) with the corresponding 95% CI.

	Vickers Hardness (GPa)		Fracture Toughness ($MPa.m^{1/2}$)		Weibull Modulus (m)		Characteristic Stress (MPa)	
	Immediate	Aged	Immediate	Aged	Immediate	Aged	Immediate	Aged
ZTA	15.94 Aa (15.31–16.58)	15.60 Aa (15.06–16.15)	3.92Aa (3.84–4.00)	4.07Aa (3.98–4.16)	6.49 Aa (5.09–8.27)	5.99 Aa (4.66–7.70)	955 Aa (910–1,003)	1,048 Aa (955–1,105)
3Y-TZP	13.17 Ab (12.53–13.81)	13.12 Ab (12.57–13.66)	4.65Ab (4.59–4.71)	4.92Bb (4.86–4.98)	7.5 Aa (5.96–9.45)	6.08 Aa (4.86–7.62)	1,340.42 Ab (1,284.8–1,398.45)	1,067.9 Ba (1,013.68–1,125.01)

Uppercase letters denote statistically significant differences between immediate and aged conditions. Lowercase letters denote significant differences between materials.

nucleation and growth mechanism associated with phase transformation and LTD. (Chevalier et al., 2009c) In contrast, conventional 3Y-TZP presented a significant phase transformation after aging (immediate: 1% and aged: 12%). Behavior that demonstrates the higher susceptibility to LTD in pure zirconia compared to zirconia-based polycrystalline composites.

High-purity alumina usually presents higher hardness than zirconia, consequently, ZTA composites hardness tends to proportionally decrease as the percentage of zirconia increases, obeying the rule of mixtures (Sequeira et al., 2017; Sarkar et al., 2007). In the current study, the experimental ZTA composite has shown Vickers hardness values of approximately 15 GPa, irrespective of aging condition. Comparable values have been observed for similar compositions of ZTA, which were higher than zirconia and lower than alumina isolated counterparts (Sequeira et al., 2017; Sarkar et al., 2007). The suitable results of the experimental ZTA is reasonable considering the direct relationship between hardness, microstructure and densification (Sequeira et al., 2017). As expected, pure zirconia presented a superior fracture toughness when compared to ZTA due to the high alumina content forming the composite matrix. However, fracture toughness remained stable in the ZTA composite after aging, while pure zirconia demonstrated a significant increase due to the compression stress generated by t-m phase transformation.

In terms of characteristic stress, the conventional 3Y-TZP used in the present study as a control group, presented a high performance (~1,340 MPa), however these high values were severely affected by hydrothermal aging in autoclave, with a significant reduction in aged condition (~1,068 MPa). Is noteworthy that after LTD simulated aging pure zirconia presented an increase in fracture toughness and a significant decrease in characteristic stress, most probably due to the phase transformation phenomena and the volumetric changes in the zirconia grains. While t-m transformation increases the fracture toughness and limits the crack propagation, it can be hypothesized that the volumetric alterations led to tension accumulation to reach the critical value, which compromised the integrity of 3Y-TZP microstructure in areas where initially there were no defects, and might explain the decrease in the mechanical behavior of the material after aging (Chevalier et al., 2007a, 2009a; Nemli et al., 2012). Despite the predominant alumina content, the experimental ZTA composite presented a characteristic stress similar to the control group (~1000 MPa), and strength maintenance after accelerated hydrothermal aging. Literature on the orthopedic field has also shown advantageous flexural strength for ZTA concentrations raging from 10, 20–30% of Y-TZP disperse phase within an alumina matrix (620, 980 and 1,000 MPa, respectively) (Casellas et al., 1999; Pezzotti et al., 2010; Tang et al., 2012), which is significantly higher than pure alumina (~500 MPa) and similar to previous findings reported for 3Y-TZP (1,000–1,200 MPa) (Sequeira et al., 2017; Tang et al., 2012; Nakamura et al., 2016). Such an advantageous mechanical performance of the ZTA composite may lie on a window into the composition and reinforcement volume fraction, fabrication process and obtained microstructure, as well as toughening mechanisms, including stress-induced phase transformation that hampers crack propagation and crack deflection through residual compressive stress resulting from the thermal expansion mismatch of the two crystalline phases (Tang et al., 2012).

Considering the ISO 6872:2015 flexural strength recommendation for fixed dental prostheses, the probability of survival of the ZTA composite estimated at 300 (100%) and 500 (99%) MPa makes the experimental ZTA composite an interesting material for anterior and posterior three-unit FDP frameworks, with the potential of being more stable to LTD compared to 3Y-TZP and less challenging esthetically than metallic frameworks. However, our prediction at the stress demanded for 4-unit or larger span FDP frameworks, 800 MPa (73–82%), suggests that different proportions and syntheses protocols of ZTA composites should be developed and characterized to improve their strength and reliability. In contrast, the probability of survival of the conventional 3Y-TZP

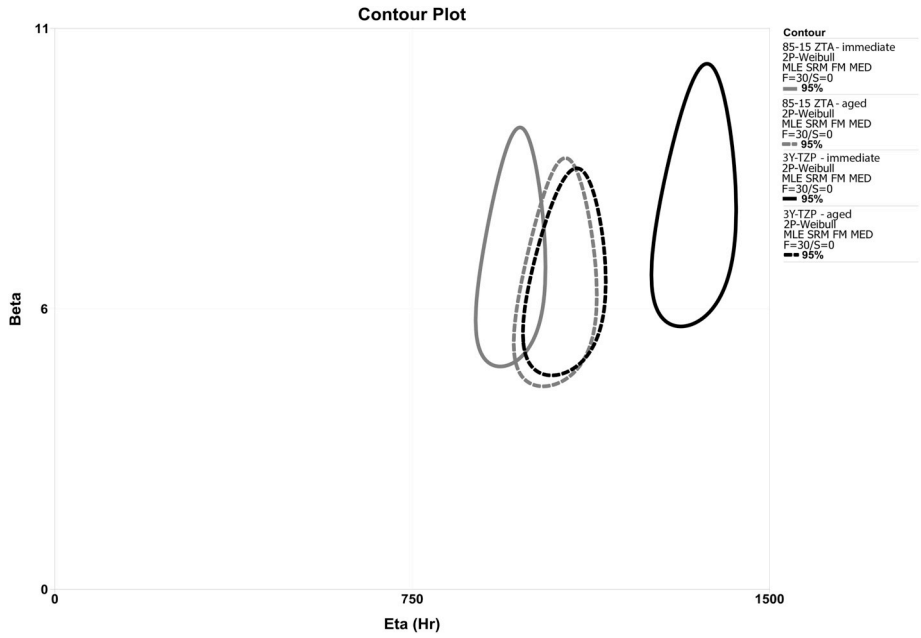

Fig. 3. Contour plot showing the relationship between Weibull modulus (m) and Characteristic stress (MPa). The overlap between conditions indicates they are statistically homogeneous (95% CI).

Table 4
Reliability and the respective 95% confidence intervals (CI).

	300 MPa		500 MPa		800 MPa	
	Immediate	Aged	Immediate	Aged	Immediate	Aged
ZTA	1.0 Aa (1.0–1.0)	1.0 Aa (1.0–1.0)	0.99 Aa (0.95–1.0)	0.99 Aa (0.96–1.0)	0.73 Ba (0.60–0.82)	0.82 Ba (0.7–0.9)
3Y-TZP	1.0 Aa (1.0–1.0)	1.0 Aa (1.0–1.0)	1.0 Aa (1.0–1.0)	0.99 Aa (0.97–1.0)	0.98 Ab (0.94–0.99)	0.84 Bb (0.76–0.91)

Uppercase letters denote statistically significant differences between missions. Lowercase letters denote significant differences between materials.

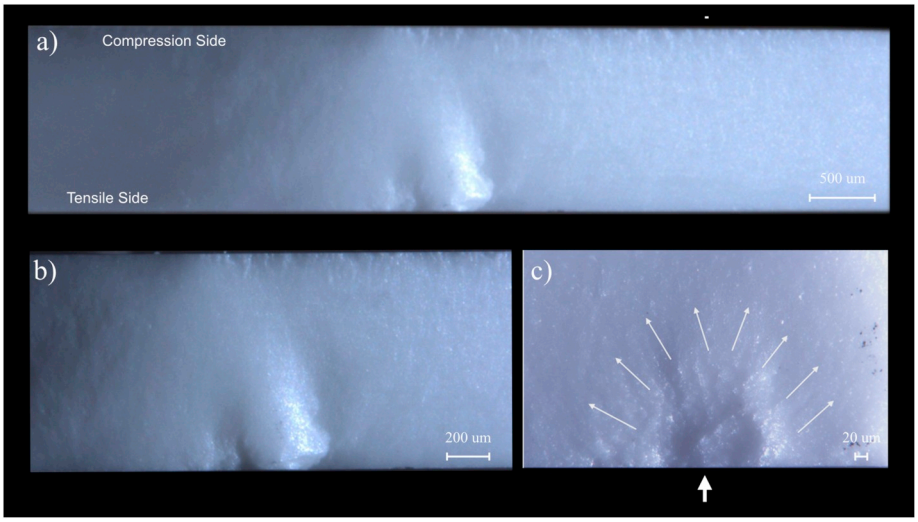

Fig. 4. Optical microscope images of a representative fractured surface. a) Identification of compression and tensile sides. b) Central area of the fragment depicting the presence of a flaw in the area subjected to maximum tensile stress. c) Suggested fracture origin and direction of propagation (arrows).

control group was estimated at 100% for 300, 500, and 800 MPa missions. However, the significant decrease in the probability of survival (up to 20%) for missions at 800 MPa sustain the concerns previously discussed about hydrothermal instability of pure zirconia submitted to low temperatures, stress and humid conditions.

The structural reliability of ceramics is an important aspect for lifetime estimation. Weibull modulus is used to describe the variation in strength values as a result of flaw population. The higher the Weibull modulus, the more homogeneous the flaw size distribution and the less the data scatter and, therefore, greater structural reliability (Quinn and Quinn, 2010; Ritter, 1995). The Weibull modulus of the experimental ZTA composite has ranged from approximately 5 to 8, which was similar

to 3Y-TZP control group (4–9) and within the range of values (5–15) reported for the currently available ceramic systems (Tinschert et al., 2000). Also, previous studies have reported an enhanced structural reliability in reinforcing an alumina matrix with homogeneously distributed zirconia particles relative to pure alumina (Tang et al., 2012).

Regarding optical properties, the experimental ZTA composite has shown a high contrast ratio (CR) and low translucency parameter (TP), without a significant influence of the laboratory aging. Intrinsic microstructural features and their interaction with light dictates the level of translucency or opacity of a determined material, such as grain size, pores and defects, refractive index mismatch between the two crystalline phases, aging, and birefringent nature of noncubic crystals with anisotropic light scattering (Zhang, 2014; Walczak et al., 2019). The experimental ZTA composite opacity may be related to the prevalence of anisotropic noncubic crystals and presence of a secondary crystal phase, as well as, the maintenance of the ZTA optical properties after artificial aging, a consequence of crystalline content and microstructure preservation due to limited zirconia phase transformation (Zhang, 2014; Vagkopoulou et al., 2009). The control group of the present study, 3Y-TZP, evidenced a tendency to increase its translucency parameter and to decrease its contrast ratio as a consequence of LTD. Hence, ZTA stability may favor long-term esthetic results after porcelain veneering, since hydrothermal aging of 3Y-TZP may increase zirconia translucency over time. Previous studies have also shown esthetically unacceptable color alterations for monolithic zirconia after approximately 3–4 years of prostheses placement (Kim and Kim, 2018).

The present results of biaxial flexural strength, Vickers hardness and fracture toughness, and high opacity and masking ability support ZTA application as a surrogate for metal and zirconia frameworks in clinical scenarios of high functional demand and darkened substrates, such as colored teeth or titanium implant abutments. Further researches on ZTA fatigue performance, as well as, biological properties are warranted.

5. Conclusion

The synthesis of the experimental zirconia-toughened alumina (ZTA) composite in a weight ratio of 85% alumina and 15% zirconia presented a dense microstructure with the reinforced zirconia particles dispersed homogeneously in the alumina matrix. The stability of optical and mechanical properties after aging encourages future research to validate its potential use as an alternative to metal and zirconia in large span prosthetic reconstructions.

Declaration of competing interest

The authors declare that they have no known competing financial interests or personal relationships that could have appeared to influence the work reported in this paper.

CRediT authorship contribution statement

E.B. Benalcázar Jalkh: Conceptualization, Methodology, Investigation, Formal analysis, Writing - original draft. **E.T.P. Bergamo:** Conceptualization, Investigation, Formal analysis, Writing - original draft, Writing - review & editing. **K.N. Monteiro:** Validation, Methodology, Investigation, Data curation, Writing - review & editing. **P.F. Cesar:** Conceptualization, Methodology, Validation, Supervision, Resources, Formal analysis, Writing - review & editing. **L.A. Genova:** Conceptualization, Methodology, Validation, Investigation, Resources, Supervision, Formal analysis, Writing - review & editing. **A.C.O. Lopes:** Methodology, Investigation, Data curation, Validation, Writing - review & editing. **P.N. Lisboa Filho:** Conceptualization, Methodology, Resources, Formal analysis, Writing - original draft, Writing - review & editing. **P.G. Coelho:** Conceptualization, Methodology, Resources, Supervision, Writing - review & editing. **C.F. Santos:** Conceptualization, Funding acquisition, Formal analysis, Writing - review & editing. **F. Bortolin:** Investigation, Visualization, Data curation, Formal analysis, Writing - original draft. **M.M.T. Piza:** Investigation, Visualization, Data curation, Formal analysis, Writing - original draft. **E.A. Bonfante:** Conceptualization, Formal analysis, Funding acquisition, Methodology, Project administration, Resources, Supervision, Writing - original draft.

Acknowledgments

To grant #2012/19078-7 São Paulo Research Foundation (FAPESP), EMU 2016/18818-8, and To Conselho Nacional de Desenvolvimento Científico e Tecnológico (CNPq), grants #304589/2017-9 and 434487/2018-0 and Capes financial code 001. Also, to FAPESP scholarships #2016/24165-7; 2016/18657-4; 2016/17793-1; 2017/19362-0; 2018/03072-6; 2019/00452-5, 2019/14798-0 and 2019/08693-1.

References

Anstis, G.R., Chantikul, P., Lawn, B.R., Marshall, D.B., 1981. A critical evaluation of indentation techniques for measuring fracture toughness: I, direct crack measurements. J. Am. Ceram. Soc. 64 (9), 533–538.
Casellas, D., Rafols, I., Llanes, L., Anglada, M., 1999. Fracture toughness of zirconia–alumina composites. Int. J. Refract. Metals Hard Mater. 17 (1), 11–20.
Chevalier, J., 2006. What future for zirconia as a biomaterial? Biomaterials 27 (4), 535–543.
Chevalier, J., Gremillard, L., 2009. Ceramics for medical applications: a picture for the next 20 years. J. Eur. Ceram. Soc. 29 (7), 1245–1255.
Chevalier, J., Cales, B., Drouin, J.M., 1999. Low-temperature aging of Y-TZP ceramics. J. Am. Ceram. Soc. 82 (8), 2150–2154.
Chevalier, J., Gremillard, L., Deville, S., 2007a. Low-temperature degradation of zirconia and implications for biomedical implants. Annu. Rev. Mater. Res. 37, 1–32.
Chevalier, J., Gremillard, L., Deville, S., 2007b. Low-temperature degradation of Zirconia and implications for biomedical implants. Annu. Rev. Mater. Res. 37, 1–32.
Chevalier, J., Gremillard, L., Virkar, A.V., Clarke, D.R., 2009a. The tetragonal-monoclinic transformation in zirconia: lessons learned and future trends. J. Am. Ceram. Soc. 92 (9), 1901–1920.
Chevalier, J., Gremillard, L., Virkar, A.V., Clarke, D.R., 2009b. The tetragonal-monoclinic transformation in zirconia: lessons learned and future trends. J. Am. Ceram. Soc. 92 (9), 1901–1920.
Chevalier, J., Grandjean, S., Kuntz, M., Pezzotti, G., 2009c. On the kinetics and impact of tetragonal to monoclinic transformation in an alumina/zirconia composite for arthroplasty applications. Biomaterials 30 (29), 5279–5282.
Daou, E.E., 2014. The zirconia ceramic: strengths and weaknesses. Open Dent. J. 8, 33–42.
Denry, I., Kelly, J.R., 2008. State of the art of zirconia for dental applications. Dent. Mater. : Off. Publ. Acad. Dental Mater. 24 (3), 299–307.
Fabbri, P., Piconi, C., Burresi, E., Magnani, G., Mazzanti, F., Mingazzini, C., 2014. Lifetime estimation of a zirconia-alumina composite for biomedical applications. Dent. Mater. : Off. Publ. Acad. Dental Mater. 30 (2), 138–142.
Fukushima, K.A., Sadoun, M.J., Cesar, P.F., Mainjot, A.K., 2014. Residual stress profiles in veneering ceramic on Y-TZP, alumina and ZTA frameworks: measurement by hole-drilling. Dent. Mater. : Off. Publ. Acad. Dental Mater. 30 (2), 105–111.
Garvie, R.C., Hannink, R.H., Pascoe, R.T., 1975. Ceramic steel. Nature 258 (5537), 703–704.
Gracis, S., Thompson, V.P., Ferencz, J.L., Silva, N.R., Bonfante, E.A., 2015. A new classification system for all-ceramic and ceramic-like restorative materials. Int. J. Prosthod. 28 (3), 227–235.
International-Standard-Organization, 2015. International Standard ISO 6872: Dentistry-Ceramic Materials. ISO.
Jiang, L., Liao, Y., Wang, C., Lu, J., Zhang, J., 2013. Low temperature degradation of alumina-toughened zirconia in artificial saliva. J. Wuhan Univ. Technol.-Materials Sci. Ed. 28 (4), 844–848.
Karihaloo, B.L., 1991. Contribution of t→ m phase transformation to the toughening of ZTA. J. Am. Ceram. Soc. 74 (7), 1703–1706.
Kim, H.K., Kim, S.H., 2018. Effect of hydrothermal aging on the optical properties of precolored dental monolithic zirconia ceramics. J. Prosthet. Dent.
Krell, A.H., Klimke, T., J, 2007. Transparent ceramics for structural applications: part 1. Physics of light transmission and technological consequences. Ceram. Forum Int. 84 (4), 41–50.
Lange, F.F., 1982. Transformation toughening. J. Mater. Sci. 17 (1), 247–254.
Lopes, A.C.O., Coelho, P.G., Witek, L., Jalkh, E.B.B., Gênova, L.A., Monteiro, K.N., et al., 2019. Nanomechanical and microstructural characterization of a zirconia-toughened alumina composite after aging. Ceram. Int.
Nakamura, K., Harada, A., Ono, M., Shibasaki, H., Kanno, T., Niwano, Y., et al., 2016. Effect of low-temperature degradation on the mechanical and microstructural properties of tooth-colored 3Y-TZP ceramics. J. Mechan. Behav. Biomed. Mater. 53, 301–311.
Nemli, S.K., Yilmaz, H., Aydin, C., Bal, B.T., Tiras, T., 2012. Effect of fatigue on fracture toughness and phase transformation of Y-TZP ceramics by X-ray diffraction and Raman spectroscopy. J. Biomed. Mater. Res. B Appl. Biomater. 100 (2), 416–424.

Pecharroman, C., Bartolomé, J.F., Requena, J., Moya, J.S., Deville, S., Chevalier, J., et al., 2003. Percolative mechanism of aging in zirconia-containing ceramics for medical applications. Adv. Mater. 15 (6), 507–511.
Pecharromán, C., Bartolomé, J.F., Requena, J., Moya, J.S., Deville, S., Chevalier, J., et al., 2003. Percolative mechanism of aging in zirconia-containing ceramics for medical applications. Adv. Mater. 15 (6), 507–511.
Pereira, G.K., Venturini, A.B., Silvestri, T., Dapieve, K.S., Montagner, A.F., Soares, F.Z., et al., 2015. Low-temperature degradation of Y-TZP ceramics: a systematic review and meta-analysis. J. Mechan. Behav. Biomed. Mater. 55, 151–163.
Pereira, G.K., Muller, C., Wandscher, V.F., Rippe, M.P., Kleverlaan, C.J., Valandro, L.F., 2016. Comparison of different low-temperature aging protocols: its effects on the mechanical behavior of Y-TZP ceramics. J. Mechan. Behav. Biomed. Mater. 60, 324–330.
Pezzotti, G., Saito, T., Padeletti, G., Cossari, P., Yamamoto, K., 2010. Nano-scale topography of bearing surface in advanced alumina/zirconia hip joint before and after severe exposure in water vapor environment. J. Orthop. Res. : Off. Publ. Orthop. Res. Soc. 28 (6), 762–766.
Piconi, C., Maccauro, G., Pilloni, L., Burger, W., Muratori, F., Richter, H.G., 2006. On the fracture of a zirconia ball head. J. Mater. Sci. Mater. Med. 17 (3), 289–300.
Pieralli, S., Kohal, R.J., Rabel, K., von Stein-Lausnitz, M., Vach, K., Spies, B.C., 2018. Clinical outcomes of partial and full-arch all-ceramic implant-supported fixed dental prostheses. A systematic review and meta-analysis. Clin. Oral Implants Res. 29 (Suppl. 18), 224–236.
Quinn, J.B., Quinn, G.D., 2010. A practical and systematic review of Weibull statistics for reporting strengths of dental materials. Dent. Mater. : Off. Publ. Acad. Dental Mater. 26 (2), 135–147.
Ritter, J.E., 1995. Predicting lifetimes of materials and material structures. Dent. Mater. : Off. Publ. Acad. Dental Mater. 11 (2), 142–146.
Sailer, I., Makarov, N.A., Thoma, D.S., Zwahlen, M., Pjetursson, B.E., 2016. Corrigendum to "All-ceramic or metal-ceramic tooth- supported fixed dental prostheses (FDPs)? A systematic review of the survival and complication rates. Part I: single crowns (SCs)" [Dental Materials 31 (6) (2015) 603-623]. Dent. Mater. : Off. Publ. Acad. Dental Mater. 32 (12), e389–e390.
Sailer, I., Strasding, M., Valente, N.A., Zwahlen, M., Liu, S., Pjetursson, B.E., 2018a. A systematic review of the survival and complication rates of zirconia-ceramic and metal-ceramic multiple-unit fixed dental prostheses. Clin. Oral Implants Res. 29 (Suppl. 16), 184–198.
Sailer, I., Balmer, M., Husler, J., Hammerle, C.H.F., Kanel, S., Thoma, D.S., 2018b. 10-year randomized trial (RCT) of zirconia-ceramic and metal-ceramic fixed dental prostheses. J. Dent.
Sarkar, D., Adak, S., Chu, M.C., Cho, S.J., Mitra, N.K., 2007. Influence of ZrO2 on the thermo-mechanical response of nano-ZTA. Ceram. Int. 33 (2), 255–261.
Sequeira, S., Fernandes, M., Neves, N., Almeida, M., 2017. Development and characterization of zirconia–alumina composites for orthopedic implants. Ceram. Int. 43 (1), 693–703.
Tang, D., Lim, H.-B., Lee, K.-J., Lee, C.-H., Cho, W.-S., 2012. Evaluation of mechanical reliability of zirconia-toughened alumina composites for dental implants. Ceram. Int. 38 (3), 2429–2436.
Tholey, M.J., Berthold, C., Swain, M.V., Thiel, N., 2010. XRD2 micro-diffraction analysis of the interface between Y-TZP and veneering porcelain: role of application methods. Dent. Mater. : Off. Publ. Acad. Dental Mater. 26 (6), 545–552.
Tinschert, J., Zwez, D., Marx, R., Anusavice, K.J., 2000. Structural reliability of alumina-, feldspar-, leucite-, mica- and zirconia-based ceramics. J. Dent. 28 (7), 529–535.
Vagkopoulou, T., Koutayas, S.O., Koidis, P., Strub, J.R., 2009. Zirconia in dentistry: Part 1. Discovering the nature of an upcoming bioceramic. Eur. J. Esthetic Dent. : Off. J. Euro. Acad. Esthetic Dent. 4 (2), 130–151.
Walczak, K., Meissner, H., Range, U., Sakkas, A., Boening, K., Wieckiewicz, M., et al., 2019. Translucency of zirconia ceramics before and after artificial aging. J. Prosthodont. 28 (1), e319–e324.
Wang, J., Stevens, R., 1989. Zirconia-toughened alumina (ZTA) ceramics. J. Mater. Sci. 24 (10), 3421–3440.
Zhang, Y., 2014. Making yttria-stabilized tetragonal zirconia translucent. Dent. Mater. 30 (10), 1195–1203.
Zhang, Y., Lawn, B.R., 2017. Novel zirconia materials in dentistry. J. Dent. Res. 22034517737483.